

AN ARTIFICIAL EAR TO ASSESS OBJECTIVE INDICATORS RELATED TO THE ACOUSTICAL COMFORT DIMENSION OF EARPLUGS: VALIDATION OF A VIBRO ACOUSTIC MODEL FOR INSERTION LOSS AND OCCLUSION EFFECT ASSESSMENT

Bastien Poissenot-Arrigoni, Simon Benacchio

École de technologie supérieure, Montréal, Québec, Canada

email: bastien.poissenot.1@ens.etsmtl.ca

Franck Sgard

IRSST, Montréal, Québec, Canada

Olivier Doutres

École de technologie supérieure, Montréal, Québec, Canada

email: olivier.doutres@etsmtl.ca

Hearing protection devices (HPD) are widely used to prevent noise-induced hearing loss (NIHL). In a noisy environment, wearing a correctly fitted HPD during all the time exposure is the sine qua non condition to prevent NIHL. However, this condition is often unfulfilled due to the discomforts induced by HPDs. Although this is a well-known fact, it remains challenging to quantify HPD comfort since it is a multidimensional concept related to subjective feelings of the users. Thus, it is necessary to use objective indicators correlated to subjective attributes of HPD comfort to help manufacturers designing efficient protectors. For earplugs, the insertion loss (IL), attenuation and occlusion effect (OE) seem good candidates to objectively describe attributes belonging to the acoustical dimension of comfort. However, most of the current ear simulators are not adapted to evaluate the physical variables related to these indicators since they do not consider important features of the external ear such as the complex earcanal geometry. As part of an ongoing project aiming at developing augmented artificial heads for measuring indicators of the acoustical comfort induced by earplugs, the goal of this study is to find parameters of the ear that significantly affect its vibro-acoustical behavior and evaluate a 3D vibro-acoustic finite element model of an artificial ear presented in a companion paper. The artificial ear is placed in anechoic conditions and excited both acoustically and mechanically. Sound pressure is measured at the eardrum location when the earcanal is open or occluded with a specially designed steel earplug and measurement are compared with numerical simulations. This study provides solid bases to the elaboration of augmented artificial ears for earplug comfort assessment.

Keywords: Artificial Ear, Comfort, Insertion Loss, Occlusion Effect

1. Introduction

A quick and repeatable way to objectively determine the attenuation of earplugs (EP) is to use acoustical test fixtures (ATF) [1]. The ATF method described in the ANSI/ASA 12.42 [2] can be used to measure insertion loss (IL) of hearing protection devices either in impulsive or continuous noise. This method is based on the utilization of a manikin of shape and size representative of certain elements of the average geometry of a human head, pinnae and earcanal. Ideally, the perfect ATF would eliminate the need of subjects to perform acoustic measurement on EPs and could be used as a designing tool by manufacturers. EPs efficiency depend on attributes of the acoustical dimension of comfort [3,4] such as the occlusion effect (OE), the intelligibility, and the over- and under-protection. Some of those comfort attributes like under- and over-protection are linked to the attenuation of EPs. However, most of commercially available ATFs have been designed to test devices such as hearing aids or headphones and are less suitable for the study of EPs. A limitation of most of existing ATFs regarding to the EP evaluation is that they cannot capture the inter-subject variability of the hearing protection device global attenuation quantified through the single number rating called “Noise Reduction Ratio” (NRR) measured on a panel of subjects. Particularly for EP, there is a significant dispersion of NRR around the mean when measured on a panel of subjects, mainly due to earcanal geometry. Indeed, the fact that a real earcanal center axis is curvilinear and that its cross-section shape varies along this curvilinear axis can affect the fit quality and the radial compression of deformable EPs such as roll-down foam protectors. The fit quality is responsible for acoustic leaks that reduce attenuation at low frequencies. The radial compression affects both EP fit and sound transmission properties and thereby sound attenuation [5-7]. Therefore, ATFs with straight earcanals are unlikely to capture both the intra- and inter-individual variability of NRR and should not be used as a design tool that accounts for a realistic EP fit. Also, in order to capture as close as possible the acoustic behavior of a human occluded ear, the earcanal of the ATF must include a silicone layer that mimics the earcanal tissues [8] and must be heated [2]. Existing ATFs which fulfill this last requirement such as the GRAS 45CB have only a portion of the earcanal which is covered with silicone. Indeed, to simulate the impedance of the tympanic membrane, ATFs (e.g. GRAS 45CB, B&K Type 4128D) are equipped with ear simulators, which are designed to represent the acoustic impedance of the tympanic membrane, plus a portion of the earcanal [9,10]. Therefore, the ear canal ends with a circumferential rigid part corresponding to the acoustic coupler rigid wall. This greatly limits the EP insertion depth that can be tested with such artificial earcanals. Some other features are missing to the ATFs available on the market to properly evaluate the OE [1]. Indeed, there are several methods to generate OE in an earcanal (like speaking, chewing or using a bone transducer), but in fine, the OE origins from the mechanical vibrations of tissues surrounding the earcanal. Therefore, it is likely that the absence on current ATFs of realistic tissues surrounding the earcanal such as temporal bone and cartilage does not make it possible to capture a realistic propagation of vibrations from the source to the earcanal skin through tissues. Consequently, there is a need to develop more realistic ATFs that mimic properly the earcanal/EP system for both acoustical and mechanical excitations. For this purpose, an artificial ear with a complex geometry and including surrounding tissues has been developed and is presented in a companion paper [11].

The study presented here is part of the development of this artificial ear and aims at finding key parameters of the ear that significantly affect its vibro-acoustical behavior. Previous works [5,6,12] have shown the benefit of finite element (FE) numerical models to better understand the vibro-acoustic behaviour of ears excited both acoustically and mechanically. Thus, a 3D vibro-acoustic FE model of the artificial ear is developed and evaluated for both acoustical and mechanical excitations. Numerical simulations are evaluated by comparisons with measurements conducted on the artificial ear.

2. Methodology

In this section the design and fabrication steps of both the artificial ear and corresponding FE model are presented. The experimental setup and numerical modelling used respectively to measure and compute the acoustic pressure at the eardrum of both the opened and occluded artificial ear and FE model are also detailed.

2.1 Artificial ear

Only a brief overview of the fabrication of the artificial ear is described here; the detailed procedure can be found in [11,13]. The geometry of the left ear of a 28 years old male subject with no outer ear pathology has been reconstructed from medical images. Three different regions of his ear were segmented: (i) the soft tissues (a single region containing skin, adipose tissue, blood vessel...), (ii) the cartilage surrounding the lateral part of the ear canal and (iii) the bony part surrounding the medial part of the ear canal. Based on the three segmented regions, a 3D computed-aid designed (CAD) geometry (Fig. 1.a) was prepared and used to build the FE model (Fig. 1.b and 2). The same CAD geometry has been used by the company True Phantom Solutions (*Windsor, Canada*) to build the artificial ear (Fig. 1.c).

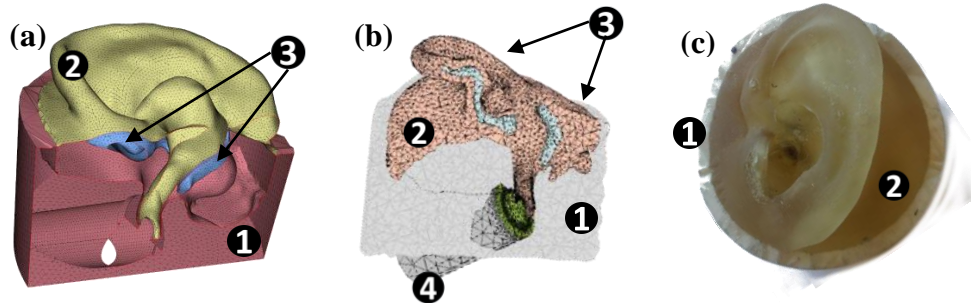


Figure 1: (a) CAD geometry of the ear, (b) FE model and (c) artificial ear - (1) bony part, (2) soft tissues, (3) cartilage and (4) aluminium insert.

Mechanical properties of soft tissues and cartilage of the artificial ear have been determined in laboratory with quasi-static mechanical analysis and material properties of bone and EP have been extracted from manufacturer data and literature [12] and are given Table 1.

A hollow cylindrical aluminum insert passes through the bony part of the artificial ear from the medial plane to the tympanic membrane (Figs. 1.a, 1.b and 3). This makes it possible to fix a quarter inch microphone which plays the role of a rigid tympanic membrane without passing any cable between the EP and the ear canal, which could be a source of acoustic leaks (see next subsection for more details on the impact of leaks around the EP). This artificial ear is a prototype and its robustness has not been taken into account in its design phase. Consequently, it includes very thin regions of skin between cartilage and the ear canal which are source of fragility and can degrade during experiments under the cumulative effects of occluding the ear with different EPs. Multiple solutions are currently investigated in order to make the artificial ears more robust. The one used in this work is to remove the cartilage and replace it by soft tissues. This solution has two advantages: (i) it completely eliminates thin regions of soft tissues that are sources of fragility and (ii) it simplifies the composition of the artificial ear (and so its associated FE model). As this work is a preliminary study, another important simplification on the artificial ear is carried out: the tympanic membrane is simplified to an acoustically rigid surface in both artificial ear and FE model.

2.2 Earplug

In order to evaluate the anatomical phantom and the numerical model, an EP has been specially designed. The EP is a steel cylinder which allows for (i) limiting the numerical modelling complexity since both EP geometry and material properties are known accurately (which won't be the case if a commercial EP were used) and (ii) assessing the self-insertion loss of the artificial ear (if one can consider that the EP provide a sufficient airtight occlusion).

The counterpart of having such a rigid EP is that it is likely to generate a larger earcanal deformation when compared to a commercial EP (like a roll-down foam EP for example). This deformation and the compression of tissues around the EP have not been taken into account in the numerical model. Several diameters of EPs have been tested in order to find the smallest diameter providing a maximal attenuation resulting to the selection of an 8 mm diameter EP.

3. Artificial ear FE model

The configuration of interest is shown in Fig.2. The ear is placed at the centre of an air-filled sphere. Its geometry is the one described in section 2.1 and the position of the EP in the numerical model has been empirically determined by observing its location during measurements. The structural boundary conditions of the ear are chosen "free". A perfectly matched layer surrounding the air-filled sphere makes it possible to simulate a free field condition. The coupling between air and solid structures is obtained by ensuring the continuity of normal acceleration and stress vector at the fluid-structure interface. The acoustical excitation is a point source of unit volume flow rate placed at 18 cm in front of the ear. The mechanical excitation is an imposed unit point force and applied on the medial plan of the bone cylinder. The coupled fluid-structure equations are solved in the frequency domain between 100 and 5000 Hz in the case of the acoustical excitation and between 100 and 2000 Hz (which is usually the frequency range where the OE is positive) in the case of the mechanical excitation.

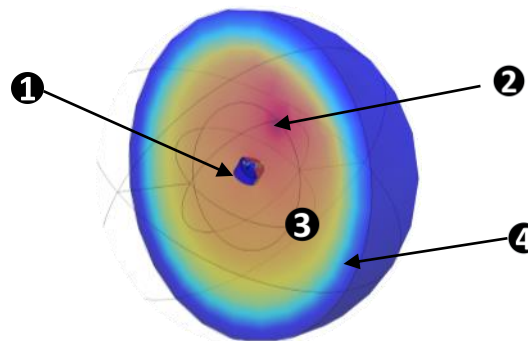


Figure 2: FE model of the artificial ear excited acoustically. (1) artificial ear, (2) point source, (3) air filled sphere (4) perfectly matched layer.

All domains were first meshed according to a convergence criterion of 6 elements per wavelength at the maximum frequency of the spectrum using quadratic tetrahedral. The 3D FE model is solved using the software *COMSOL Multiphysics 5.4* (*COMSOL*[®], *Stockholm, Sweden*). Ultimately, the acoustic pressure at the eardrum predicted with this model is to be compared with the acoustical pressure measured on the artificial ear. Mechanical properties of the ear are summarized in Table 1.

Table 1: Mechanical properties of the artificial ear

	Bone	Soft tissues	EP (AISI 4140)
Young modulus [kPa]	13.6×10^6	203	200×10^6
Loss factor []	0.01	0.045	0.001
Poisson ratio []	0.31	0.28	0.3
Density[kg.m ⁻³]	2267	1007	7850

4. Experimental setups

Two experimental setups have been designed to evaluate the FE model shown in Fig. 2: one for acoustical excitation and one for mechanical excitation. For both experimental setups, the “free structural boundary condition” is obtained suspending the artificial ear to a low-stiffness spring in an anechoic chamber. In the case of the acoustical excitation, a Mid High Frequency SIEMENS LMS Volume Source is placed so that the theoretical centre of the monopole source is 18 cm in front of the artificial ear (as in the numerical model) (Fig. 3.a). In the case of the mechanical excitation configuration, a TMS K2004E01 Mini SmartShakerTM is attached to the artificial ear with a steel rod (Fig. 3.b). An impedance head is mounted between the rod and the artificial ear in order to measure the force transmitted by the shaker to the artificial ear together with the acceleration at the fixation point. For both the acoustical and mechanical excitations, a white noise is generated with a Larson-Davis SRC20 signal source.

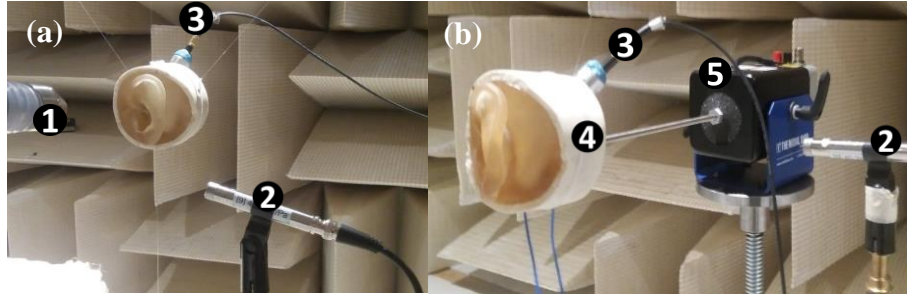


Figure 3: Measurement setup for (a) the acoustical excitation and (b) the mechanical excitation. (1) Point source, (2) reference microphone, (3) visible part of the quarter inch microphone mounted flush to the “rigid tympanic membrane” (4) impedance head (not visible on the picture), (5) shaker.

For the acoustical excitation configuration, acoustical transfer functions of the open and occluded ear ($H_{Ac,Open}$ and $H_{Ac,Occluded}$) are obtained by dividing the acoustic pressure measured with the internal quarter inch microphone (which also plays the role of a rigid tympanic membrane) by a reference acoustic pressure measured at the location of the center of the cylinder base of the artificial ear, when the artificial ear is removed. The IL is calculated from those transfer functions following:

$$IL = 20 \times \log_{10} \left(\frac{|H_{Ac,Open}|}{|H_{Ac,Occluded}|} \right). \quad (1)$$

In the case of the mechanical excitation configuration, the force measured with the impedance head is taken as reference for transfer functions of open and occluded ear ($H_{Mec,Open}$ and $H_{Mec,Occluded}$). $H_{Mec,Open}$ and $H_{Mec,Occluded}$ are thus obtained dividing the acoustic pressure measured with the internal quarter inch microphone by the force measured with the impedance head. OE is derived from those two transfer functions such as:

$$OE = 20 \times \log_{10} \left(\frac{|H_{Mec,Occluded}|}{|H_{Mec,Open}|} \right). \quad (2)$$

A reference microphone is placed close to the ear during all measurements to check the ambient noise level, and measurements are performed three times per configuration. All OE measurements have been performed after IL measurements.

5. Results and discussion

5.1 Evaluation of the FE model of the artificial ear excited acoustically

Figs. 4.a and 4.b show the experimental and numerical transfer functions of both the open and occluded ear excited acoustically together with the measured and calculated ILs respectively. In the case of the open ear canal, a fairly good agreement can be observed between the FE model and the experiment (see Fig. 4.a). There is a slight frequency shift for the resonance of the open ear canal occurring at 2340 Hz, whereas the model predicts it at 2000 Hz. This difference is attributed to a little cavity that has been machined at the end of the ear canal (in order to fix the quarter inch microphone in place of the tympanic membrane) and whose dimensions are not known precisely and thus may be inaccurately accounted for in the FE model. In the case of the occluded ear canal however, large discrepancies can be observed between the simulated and measured acoustical transfer functions resulting in a poor agreement between the measured and computed IL. The measured IL is significantly lower than the predicted one except around 250 and 2000 Hz. The potential reasons for these discrepancies are: (i) artificial ear manufacturing defects, (ii) microphone fixation at the end of the ear canal which may cause some air leaks (iii) air leaks between the EP and the ear canal, (iv) limits of the numerical model cited in sections 2.2 and 3 related to the approximate position of the EP and tissues deformation and (v) uncertainties related to the characterisation of material properties.

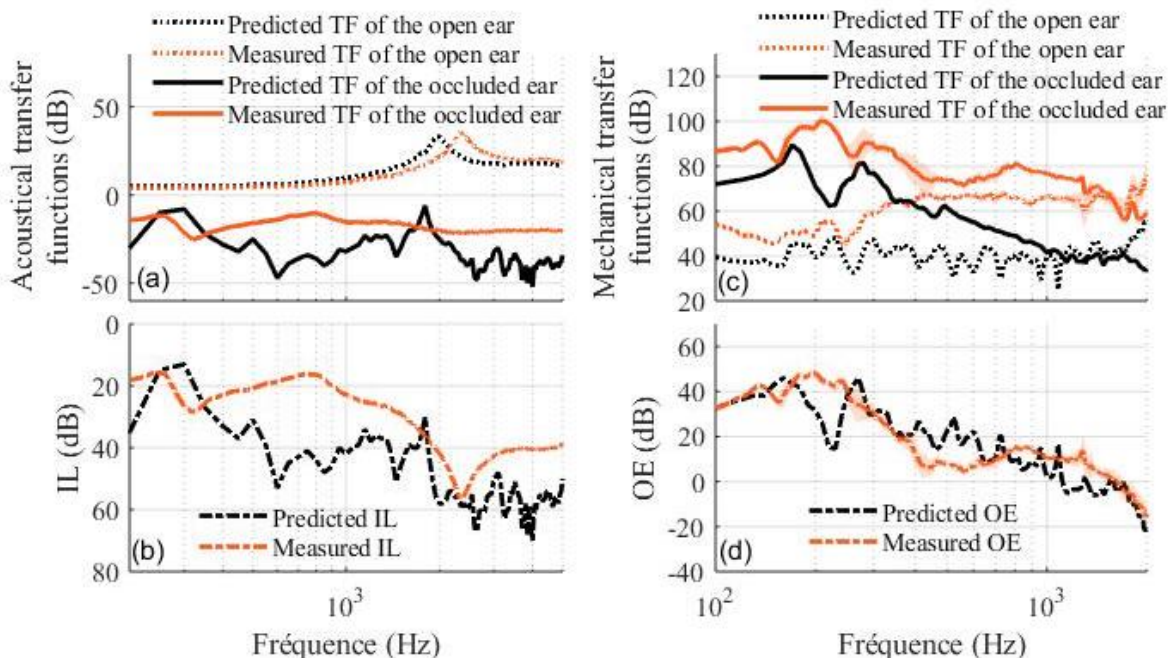


Figure 4: Experimental and numerical transfer functions (TF) of the open and occluded ear, excited acoustically (a) and mechanically (c) and derived IL (b) and OE (d).

Note that manufacturing defects are mainly air bubbles in tissues that can cause material inhomogeneity which is not taken into account in the FE model. If air bubbles are present near the ear canal they can degrade the ear canal surface and induce acoustic leaks between the EP and the ear canal.

5.2 Evaluation of the FE model of the artificial ear excited mechanically

Figs. 4.c and 4.d present the experimental and numerical transfer functions of both the open and occluded ear excited mechanically together with the measured and calculated OEs respectively. Large discrepancies can be observed between predicted and measured transfer functions. For both the opened and occluded configurations, the predicted transfer function level is lower than the measured one in the whole frequency range of interest. Air leaks at the back of the ear or between the EP and the earcanal, and inhomogeneity of materials are suspected to be responsible of these differences. Indeed, all the changes of the geometry consecutive to the fixation of the microphone flush to the tympanic membrane are not taken into account in the model. In particular, a sealing ring was used to prevent any leaks that could be caused by the microphone fixation (its efficiency must be further examined). Those modifications of geometry are very close to the measurement point, and the airborne noise radiated by the shaker was not taken into account in the numerical model and could have been captured by the quarter inch microphone at the back of the ear. This could explain why experimental transfer functions levels are higher than numerical transfer functions levels, especially in the opened earcanal configuration. Differences between predicted and measured transfer functions can also be due to the chosen mechanical excitation. The shaker installation is not straightforward and a “rigid” steel rode was used to fix the shaker to the ear. The load could thus have been transmitted to the ear in all directions and not only along the normal to the artificial ear surface as measured by the impedance head and considered in the numerical model. As mentioned by Brummund in the case of an axisymmetric FE model of an ear [12], mechanical transfer functions are very sensitive to the boundary and load conditions unlike the OE derived from those transfer functions. However, the effect of the occlusion on the level of the transfer function is correctly captured by the model resulting in a satisfactory prediction of the OE in the whole frequency range except at 200 Hz and between 400 and 600 Hz as shown in Fig. 4.d. This observation is consistent with Brummund’s results [12].

One can note fluctuations in simulated curves (Fig. 4). These fluctuations correspond to the multiple artificial ear resonance frequencies. Additional numerical simulations (not shown here) indicate that an increase of the loss factor of the artificial ear materials smoothes out these resonances. This suggests that the initial model do not capture correctly the damping in the system (especially in the open earcanal configuration as shown by mechanical transfer functions) maybe due to the uncertainties on the material properties.

6. Conclusion

In this work, a vibro-acoustic FE model of a simplified artificial ear in which cartilage has been replaced by soft tissues and excited mechanically or acoustically has been developed. The artificial outer ear of realistic geometry has been reconstructed from magnetic resonance images of a human subject and fabricated using synthetic materials mimicking the real human ear bone and soft tissues. The cartilage has been removed and replaced by soft tissues to eliminate thin regions of soft tissues that are sources of fragility, and simplify the composition of the artificial ear (and its associated FE model). A simplified steel cylinder EP has been used to evaluate this numerical model. It has been shown that, the numerical model allows for accurate prediction of the acoustic pressure of the open earcanal excited acoustically, but differences appear when the canal is occluded leading to an important overestimation of the EP insertion loss. Despite differences observed between predicted and measured transfer functions of the open and occluded ear excited mechanically, the FE model provides a satisfactory prediction of the OE. In both configurations, differences are mainly attributed to possible leaks and inhomogeneity of materials and measurement artifacts that are not taken into account in the numerical model. Further investigations must be done to either eliminate experimental leaks, or, if not possible, account for leaks in the FE model. The first solution will be preferred because in fine, this FE model is to be

calibrated and validated against measurement. The cartilage will also be added and its effect on both IL and OE will be investigated. Ultimately this artificial ear is intended to be integrated in an acoustical test fixture that makes it possible to measure acoustic indicator of EPs taking into account both the intra- and inter-individual variability.

7. Acknowledgement

Authors want to thank the Institut de Recherche Robert Sauvé en Santé et Sécurité du travail (IRSST) and MITACS for the funding of this research (grant number 2015-0014 and IT10643).

REFERENCES

1. E. H. Berger, « Preferred Methods for Measuring Hearing Protector Attenuation », in *Proceedings of the Internoise 2005*, Rio de Janeiro, Brazil, p. 4432–4441, (2005).
2. ANSI-ASA S.12.42, « Methods for the Measurement of Insertion Loss of Hearing Protection Devices in Continuous or Impulsive Noise Using Microphone-in-Real-Ear or Acoustic Test Fixture Procedures », 2nd edition, New-York (NY): American National Standards Institute and American Society of Acoustic, (2010).
3. O. Doutres, F. Sgard, J. Terroir, « A review about hearing protection comfort and its evaluation », *J. Acoust. Soc. Am.*, vol. 141, no 5, p. 4025-4025, (2017).
4. J. Terroir, O. Doutres, F. Sgard, « Towards a “global” definition of the comfort of earplugs », (2017).
5. G. Viallet, F. Sgard, F. Laville, et H. Nélisse, « Investigation of the variability in earplugs sound attenuation measurements using a finite element model », *Appl. Acoust.*, vol. 89, p. 333-344, mars (2015).
6. G. Viallet, F. Sgard, F. Laville, et J. Boutin, « A finite element model to predict the sound attenuation of earplugs in an acoustical test fixture », *J. Acoust. Soc. Am.*, vol. 136, n° 3, p. 1269-1280, (2014).
7. Berger, E.H., 'Calibrating' the insertion depth of roll-down foam earplugs, in *Proc. Mtgs. Acoust.*, 19:040002, (2013).
8. J. Schroeter, « The use of acoustical test fixtures for the measurement of hearing protector attenuation. Part I: Review of previous work and the design of an improved test fixture », *J. Acoust. Soc. Am.*, vol. 79, n° 4, p. 1065-1081, (1986).
9. IEC 60138-4 2010, *Simulators of human head and ear – Part 4: Occluded-ear simulator for the measurement of earphones coupled to the ear by means of ear inserts*, Genève, Switzerland: International Electro-technical Commission, (2010).
10. Y. Luan, F. Sgard, S. Benacchio, H. Nélisse, O. Doutres. "A coupled finite element/transfer matrix method to simulate the insertion loss of earplugs in an acoustic test fixture", in *Proceedings of the 26th International Congress on Sound and Vibration*, Montréal, (2019).
11. S. Benacchio, B. Poissenot-Arrigoni, O. Doutres, F. Sgard, "An artificial ear to assess objective indicators related to the acoustical comfort dimension of earplugs: comparison with attenuation and occlusion effect measured on subjects", in *Proceedings of the 26th International Congress on Sound and Vibration*, Montréal, (2019).
12. M. Brummund. Study of the occlusion effect induced by an earplug: modelling and experimental validation. Thèse de doctorat électronique, Montréal, École de technologie supérieure, (2014).
13. F. Sgard, S. Benacchio, Y. Luan, H. Xu, K. Carillo, O. Doutres, H. Nélisse, E. Wagnac, J. De Guise, « Vibroacoustic modeling of an in vivo human head wearing a hearing protection device using the finite element method », In *Euronoise 2018: Conference Proceedings: the 11th European Congress and Exposition on Noise Control Engineering* (Heraklion, Crete - Greece, May 27-31, p. 899-906. EAA – HELINA, (2018).